Multi-channel Interference Measurement and Modeling in Low-Power Wireless Networks

Guoliang Xing[1]; Mo Sha[2,5]; Jun Huang[1]; Gang Zhou[3]; Xiaorui Wang[4]; Shucheng Liu[5]
[1]*Michigan State University, USA;* [2]*Washington University in St. Louis, USA*
[3]*College of William and Mary, USA;* [4]*University of Tennessee, Knoxville, USA*
[5]*City University of Hong Kong, HKSAR*

***Abstract*—Multi-channel design has received significant attention for low-power wireless networks (LWNs), such as 802.15.4-based wireless sensor networks, due to its potential of mitigating interference and improving network capacity. However, recent studies reveal that the number of *orthogonal* channels available on commodity wireless platforms is small, which significantly hinders the performance of existing multi-channel protocols. A promising solution is to explore the use of *partially overlapping channels* for communications. However, this approach faces several key challenges such as increased inter-channel interference and significantly higher overhead of channel measurement. In this paper, we systematically study the inter-channel interference and its impact on link capacity and the performance of multi-channel protocols in LWNs. First, we develop empirical models for characterizing inter-channel signal attenuation based on experiments on TelosB motes. We then propose a novel measurement algorithm which can significantly reduce the overhead of multi-channel interference measurement by exploiting the spectral power density (SPD) of the transmitter. Finally, we apply our interference models to both link capacity analysis and channel assignment protocols. Our extensive experiments on a testbed of 30 TelosB motes show that our interference measurement algorithm has an average error of 2.95%. Our results also demonstrate that multi-channel protocols for LWNs can significantly benefit from using overlapping channels.**

***Keywords*-interference, measurement and modeling, overlapping channels, low-power wireless networks**

I. Introduction

Interference is a fundamental issue in wireless networks. Due to the broadcast medium, wireless transmissions from one node interfere with the reception of surrounding nodes resulting lower network throughput capacity. The situation is even worsened for *low-power wireless networks (LWNs)*, such as 802.15.4-based wireless sensor networks, which only have limited bandwidth. Understanding and mitigating interference is thus critical to the performance of such networks. This becomes a pressing issue as LWNs are being increasingly deployed for *performance-sensitive* applications, such as structural health monitoring and home entertainment, which often impose stringent requirements on system throughput and delay.

A promising approach to mitigating interference is to divide radio spectral band into sub-ranges called *channels* and assign different channels to different subsets of nodes in a network. Recently, a number of multi-channel solutions have been proposed [2][7][8][18]. However, these works assume the channels to be *orthogonal*, i.e., transmissions on different channels do not interfere with each other. However, commodity wireless platforms only have a small number of orthogonal channels. For instance, among the 11 channels of 802.11b, only 3 are orthogonal [13], as each channel has a bandwidth of 22 MHz while the spacing between adjacent channels is only 5 MHz. To address this issue, several studies [3][10][13][21] have been proposed to utilize *overlapping channels* in 802.11 networks. Although transmissions on overlapping channels may interfere with each other, they can lead to substantial improvement in network capacity when the inter-channel interference is carefully controlled [13].

Similar to the situation of 802.11, only a small number of orthogonal channels is available for 802.15.4 LWNs, which significantly hinders the performance of existing multi-channel protocols. Unfortunately, the existing efforts of utilizing overlapping channels in 802.11 networks cannot be applied to LWNs due to the following reasons.

First, the existing 802.11 inter-channel interference models [13] are not suitable for LWNs. Inter-channel interference models are essential for guiding the use of overlapping channels. Our experiments on multi-channel 802.15.4 TelosB motes reveal unique interference characteristics that cannot be captured by existing 802.11 models. Second, the current modeling approaches for overlapping channels cause prohibitively high overhead for LWNs. Several measurement-based models [6][15][16] are available for characterizing the interference in 802.11 networks. These models incur a measurement complexity of $O(M^2)$ in a multi-channel network with M overlapping channels. Such a complexity, although may be acceptable for 802.11 networks, can counteract the benefit of using overlapping channels for LWNs, whose effective bandwidth is only 10 to 100 Kbps [7][8].

In this paper, we propose a systematic approach of measuring and modeling the interference in multi-channel LWNs. To the best of our knowledge, our work is the first empirical study on inter-channel interference models and their impact on MAC design and channel assignment. Our major contributions are summarized as follows.

1) We develop empirical inter-channel interference mod-

els for LWNs based on experimental results from 802.15.4 TelosB motes. Our models characterize inter-channel signal attenuation, which serves as a basis for efficient use of overlapping channels.

2) We propose a novel lightweight mechanism for measuring inter-channel interference. By exploiting the *spectral power density (SPD)* of the transmitter, our method can efficiently measure the interference on multiple channels without requiring channel switches at the receiver. As a result, the additional overhead of using overlapping channels is significantly reduced.
3) We apply our interference models to both link capacity analysis and channel assignment protocols. By integrating inter-channel interference models, a MAC-layer model, and an existing analytical framework for modeling link capacity, we can predict the throughput of a link in the presence of multiple interferers on different channels. Moreover, our models are integrated into two latest multi-channel sensor network protocols to demonstrate a case of network throughput improvement based on overlapping channels.
4) We evaluate our approach through extensive experiments on a testbed of 30 802.15.4 TelosB motes. Our results show that our inter-channel interference models not only are accurate but also incur low measurement overhead. Our interference measurement algorithm has an average measurement error of 2.95%. Our results also demonstrate that channel assignment protocols for LWNs significantly benefit from using overlapping channels.

The rest of the paper is organized as follows. Section II reviews related work. Section III presents empirical modeling of inter-channel interferences. Section IV introduces lightweight inter-channel interference measurement. In Section V, we integrate our interference models with existing link capacity models and channel assignment protocols. Section VI presents the experimental results and Section VII concludes the paper.

II. Related Work

Interference measurement and modeling is critical for the performance of wireless networks. Son et al. [19] showed that the signal to interference and noise (SINR) model of CC1000 radio is dependent on both received signal strength (RSS) and the number of interferers. However, this result is inconsistent with more recent findings on other radio platforms (e.g., CC2420) [12][17]. Maheshwari et al. [12] showed that the physical SINR model is more accurate than other interference models, based on the experiments on telosB motes.

Recently, measurement-based interference modeling for 802.11-based wireless networks has received significant attention [6][15][16]. Compared with the existing idealistic models (e.g., the disc model), the empirical interference models proposed in these studies are more realistic and can be instantiated by radio profiling and measurements. These works focused on *intra-channel* interference measurement/modeling and do not address the issue of interference in multi-channel wireless networks.

Recently, there is increasing interest of using partially overlapped channels to improve the capacity of 802.11 networks. Fuxjager et al. [4] studied the detrimental effects of inter-channel interference on network performance through experiments. Several recent studies quantified the inter-channel interference either through measurements using spectrum analyzer [3] or analytical models of the spectral power density (SPD) [10][21]. However, none of them addressed the issue of interference modeling based on *in-situ* measurements.

Mishra et al. [13] proposed a systematic method to modeling interference of partially overlapped channels for 802.11 wireless networks. There exist several key distinctions between [13] and our work. First, the focus of [13] is *static* interference models based on radio transmit spectrum mask and channel spacing, which cannot reflect channel and environment dynamics at run time. In contrast, we focus on empirical *statistical* models that can be directly measured by nodes at run time. Second, although a simple empirical inter-channel interference model is also proposed in [13], it incurs prohibitively high measurement overhead. In this paper, we propose a novel method that significantly reduces the overhead of multi-channel interference measurement. Third, different from [13] which assumes 802.11 networks, we focus on inter-channel interference in LWNs with both static and variable transmit power, and study its impact on both low-power link capacity analysis and multi-channel protocols.

Several recent works have studied the inter-channel interference in LWNs [5][20][22]. Wu et al. [22] showed that the number of orthogonal channels on the CC2420 radio is small. Incel et al. [5] studied the influence of adjacent channel interference on the data delivery of LWNs. Toscano et al. [20] modeled the inter-channel interference of 802.15.4 radios based on signal spectral power density (SPD) function. However, these studies do not address the issue of empirical modeling of inter-channel interference based on in-situ measurements.

Multi-channel assignment has been extensively studied in 802.11 wireless networks [2][18]. Recently, several channel assignment protocols are developed for LWNs [7][8][22]. However, these protocols assume adequate number of orthogonal channels, or exclude overlapping channels in channel assignment. In this work, we demonstrate the advantage of using overlapping channels by integrating our measurement-based inter-channel interference models with a representative channel assignment protocol [22] and a multi-channel MAC protocol [8].

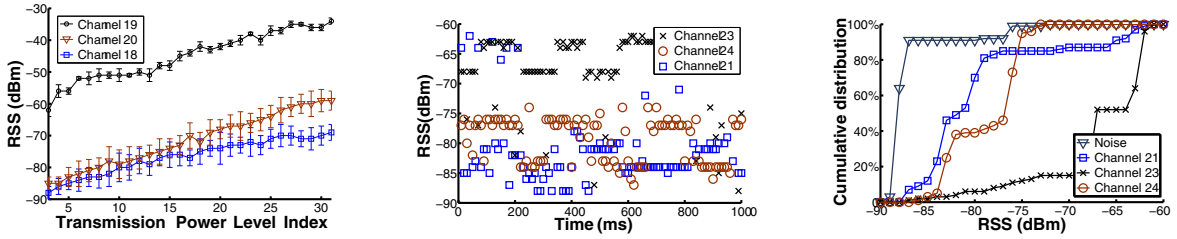

(a) Average RSS on channel 18, 19, and 20 with 90% confidence interval.

(b) RSS time series (sampled every 10ms) on channel 21, 23, and 24.

(c) The cumulative probability density of RSS on channels 21, 23, and 24.

Figure 1. RSS measured on different channels when the sender transmits on channel 19 and varies transmit power level.

III. Empirical Modeling of Inter-channel Interference

In this section, we investigate how radio signals attenuate between the sender and receiver when they operate on different channels. Based on the experimental results on TelosB motes, we develop two empirical models to quantify the relationship between transmit power and received signal strength indicator (RSSI) values measured on multiple channels. These models can be used for three purposes: 1) to enable fine-grained assessment and control of inter-channel interference; 2) to serve as the basis for a lightweight inter-channel interference measurement mechanism (Section IV); 3) to predict the link capacity in presence of interferers on multiple channels and guide the assignment of overlapping channels in multi-channel protocols (Section V).

A. Experimental methodology

Our experiments are conducted on a testbed composed of TelosB motes installed with TinyOS-2.0.2. Each mote is equipped with a 802.15.4 compliant Chipcon CC2420 radio, which has a maximum bit rate of 250 kbps. The CC2420 radio has 31 transmit power levels between -25 to 0 dBm. The Received Signal Strength Indicator (RSSI) of CC2420 contains the measurement of signal power (in the unit of dBm). 802.15.4 specifies 16 channels (numbered channel 11 to 26) in 5 MHz steps. However, the bandwidth of each channel is larger than 5 MHz, which leads to the overlap between adjacent channels.

The RSSI readings contain the signal power of both received transmissions and noise. To mitigate the impact of noise, each mote estimates the average noise strength by every 10 ms by reading the RSSI register before any transmissions. The RSSI value of an incoming packet is then subtracted by the estimated noise strength. A similar method is employed in [12].

B. Inter-channel signal attenuation

We study the correlation between transmit power of a sender and the received signal strength (RSS) measured by a receiver on different channels. In the experiments, two motes are placed in an office environment. One mote serves as the sender and transmits at the maximum rate using a fixed channel. Another mote serves as the receiver and switches between different channels. Each experiment is repeated for 10 runs. When the sender and receiver use different channels, the packets cannot be received by the receiver. The receiver reads the RSSI register every 10 ms. The noise values in the RSSI readings are then filtered out by subtracting the estimated average noise strength.

Fig. 1(a) shows RSS (with 90% confidence interval) measured by the receiver on channels 18 to 20, while the sender transmits on channel 19. The sender increases its transmit power from level 3 to 31. It can be seen that the RSS grows nearly linearly with the sender's transmit power. This result shows that a strong correlation exists between RSS and the transmit power when the channels of the sender and receiver are the same or close to each other.

Fig. 1(b) shows the RSS time series when the receiver uses channels 21, 23, and 24. The RSSI register is read every 10 ms while the sender varies the transmit power for every transmission. Surprisingly, the RSS values do *not* exhibit a strong correlation with the transmit power. For each receiver channel, the RSS values scatter within a relatively narrow region. For instance, most RSS values on channel 23 fall in the range $[-68dBm, -63dBm]$. Although the mean RSS remains around -65.6 dBm, the variance is high. This phenomenon can be explained as follows. First, by the design, the sender's signal power is mostly concentrated within a narrow frequency range and decays quickly outside of this range [1]. Therefore, even when the sender varies its transmit power, the difference in RSS observed by the receiver on a distant channel is small. Moreover, although the precision of RSSI of CC2420 is one dBm, the measurement error of RSS values could be several dBms (as shown in Fig. 1(a)). Due to the above two factors, the RSS measurement of the receiver on a distant channel has little correlation with the sender's transmit power.

Fig. 1(c) shows the cumulative probability density (CDF) of noise strength and RSS on different channels. We can see that the RSS values are much higher than the noise strength. Moreover, the CDFs of them have a narrow transitional region (around 10 dBm). We also measured the RSS on the channels (11 to 16, 25 and 26) that are distant from the sender channel. These measurements are not distinguishable from ambient noise, which suggests negligible interference.

The above experiments are repeated in a variety of

settings with different nodes' channels, different distances between sender and receiver, and both indoor and outdoor environments. The detailed results are omitted due to space limitation. Despite some variations, the following common observations can be made from our experiments: 1) The RSS grows nearly linearly with the transmit power when the sending and receiving channels are the same or close to each other; 2) When the sending and receiving channels are further apart, the RSS falls within a narrow region while no strong correlation with the transmit power is exhibited; 3) When the sending and receiving channels are far away from each other, the RSS is not impacted by the sender's transmissions.

We refer to two channels in the above three cases as *strongly*, *weakly*, and *not overlapping*, respectively. We note that although adjacent channels are always strongly correlated, two channels apart by two or three channels could be either strongly or weakly correlated. Therefore, the degree of correlation of two channels cannot be statically determined by the spacing between them. We observe that weakly correlated channels have significant impact on the packet delivery performance of a link. For example, when a sender transmits on channel 24 and a jamming node transmits on channel 22, although the two channels are weakly correlated, the packet reception ratio drops from 100% to as low as 60%.

C. Modeling inter-channel RSS

As shown in Fig. 1, the relationship between RSS and transmit power is significantly influenced by the degree of correlation between sending and receiving channels. We now present two empirical models for the interference between strongly and weakly correlated channels, respectively.

Denote $RSS(u^{(x)}, v^{(y)}, P_z)$ as the RSS measured by node v on channel y when node u transmits on channel x with power level P_z. We employ the following simple linear function to model the signal attenuation between strongly correlated channels:

$$RSS(u^{(x)}, v^{(y)}, P_z) = A_{u^{(x)},v^{(y)}} \times P_z + B_{u^{(x)},v^{(y)}} \qquad (1)$$

where $A_{u^{(x)},v^{(y)}}$ and $B_{u^{(x)},v^{(y)}}$ are two constants dependent on the physical environment and channels. We note that a similar linear model is also used in [11][17] to model the signal attenuation on the same channel. Eq. (1) does not model the variance of RSS because it is very small as shown in Fig. 1(a). The linear model in (1) can be efficiently measured for a wireless link. The sender can periodically transmit at two different power levels and the receiver then obtains the model by the linear interpolation of average RSS values measured for each transmit power level of sender.

For weakly correlated channels, the mean RSS has no statistical significance as the RSS distribution has a high variance (shown in Fig. 1(b) and Fig. 1(c)). We use a discrete quantile function (the inverse of cumulative probability density function) to capture the statistical property of the RSS distribution. Specifically, for a given quantile $\alpha \in (0, 1)$, the corresponding RSS is the value X such that the probability that an RSS measurement is less than X is α:

$$RSS(u^{(x)}, v^{(y)}, \alpha) = X \mid Prob(RSS < X) = \alpha \qquad (2)$$

The above quantile function can be easily obtained with low memory and computation overhead. We note that, despite the difference in models (1) and (2), they can be measured similarly by having the sender broadcast a number of packets while the receiver distinguish whether two channels are strongly or weakly correlated from the RSS measurements and establish the corresponding model.

IV. Lightweight Multi-channel Interference Measurement

A major challenge faced by the design of multi-channel protocols is the significant complexity incurred in measuring the conditions of multiple channels. Suppose a channel is overlapped with at most M channels. Although our inter-channel interference models (1) and (2) can be efficiently measured for two channels, they incur a complexity of $O(M^2)$ for all combinations of sender/receiver channels. In this section, we propose a lightweight measurement mechanism that significantly reduces the complexity of multi-channel interference measurement.

Denote interference set $I_u^{(x)}$ as the set of nodes that can be interfered when node u transmits on channel x. The problem of inter-channel interference measurement can be formally defined as follows. Given a node u and its interference sets of all channels, measure RSS models $RSS(u^{(x)}, v^{(y)})$ for all combinations of (x, y, v) where $v \in I_u^{(x)}$, x and y are sending and reveiving channels respectively. Note that the nodes in $I_u^{(x)}$ may not lie within the communication range of u. We assume interference sets of all channels are known *a priori*. Several existing methods [25] can be used to identify the interference set of a node.

Our mechanism exploits the characteristics of *spectral power density* (SPD) of transmitters and allow a receiver to infer the interference on different channels without actually switching between multiple channels. When a node transmits on a wireless channel, it spreads its signal power over bandwidth using specific modulation techniques such as DSSS and OFDM. SPD characterizes this sender-side signal power distribution in frequency domain. If SPD is known, we can infer the inter-channel interference without actually measuring it.

A. SPD-based measurement algorithm

Our mechanism consists of two stages: SPD measurement and multi-channel interference derivation based on SPD. For a node u, its SPD function can be obtained by conducting

spectral power analysis using special equipments such as spectrum analyzer. However such an offline approach is not only time/cost-consuming but also inaccurate as the performance of radio hardware varies over time due to aging or environmental effects. We now describe an algorithm of deriving SPD using in-situ measurements among nodes.

1) SPD measurement: Our algorithm exploits the receiver-independent characteristic of SPD to reduce measurement complexity. The basic idea is to calculate sender's SPD at the receiver based on signal *path loss*. The algorithm takes two steps to measure SPD. In the first step, *all* nodes in $\cup_x I_u^{(x)}$ measure the path loss to the sender on all channels through *intra-channel* signal attenuation modeling discussed in Section III-C. For a given node v in $I_u^{(x)}$, the path loss between u and v on channel x, denoted by $PL_x(u,v)$, can be calculated as

$$PL_x(u,v)_{dB} = P_{z\ dBm} - RSS(u^{(x)}, v^{(x)}, P_z)_{dBm} \quad (3)$$

where we abuse the notion a little by using P_z and $P_{z\ dBm}$ to represent the transmit power index (0 to 31 defined for CC2420) and the corresponding power in the unit of dBm, respectively. The mapping between P_z and $P_{z\ dBm}$ can be found in CC2420 data sheet [1]. After path loss is measured for each channel, we select a set of M nodes in I_u, then assign each channel a node for measuring *inter-channel* RSS model *simultaneously*[1]. The SPD can then be directly derived through the inverse function of inter-channel RSS models. We note that the M nodes can be randomly chosen within $I_u^{(x)}$, as the degree of overlapping (strongly or weakly) of two channels is solely determined by the SPD of node u. As we have different inter-channel RSS models for strongly and weakly overlapping channels, we now present SPD measurement for these two cases respectively.

For strongly correlated channels (x,y), we define the SPD function of sender u as $f_u(x,y,z)$, which corresponds to the signal power distributed on channel y, when u transmits on channel x using power level P_z. Assume that node v is assigned to a strongly correlated channel y, it will measure the inter-channel RSS model (Eq. (1)). We can then calculate $f_u(x,y,z)$ at the receiver by

$$f_u(x,y,z)_{dBm} = RSS(u^{(x)}, v^{(y)}, P_z)_{dBm} + PL_y(u,v) \quad (4)$$

For weakly overlapping channels, the SPD has no strong correlation with sender's transmitting power. Consistent with the definition of (2), we define the SPD function of sender u as a discrete quantile function $g_u(x,y,\alpha)$. For a given quantile $\alpha \in (0,1)$, $g_u(x,y,\alpha)$ is the value $Y_{\ dBm}$ such that the probability that the signal power distributed on channel y be less than Y_{dBm} is α, when node u transmits on channel x. Now assume that node v is assigned to weakly overlapping channel y, it will measure the inter-channel RSS model (Eq. (2)). Then using the path loss obtained in (3), we can calculate $g_u(x,y,\alpha)$ at the receiver by:

$$g_u(x,y,\alpha)_{dBm} = RSS(u^{(x)}, v^{(y)}, \alpha)_{dBm} + PL_y(u,v) \quad (5)$$

We note that the difference in the SPD derivation for strongly and weakly correlated channels does no incur additional overhead in the measurement. This is because node u does not need to distinguish whether two channels are strongly or weakly correlated when it measures different RSS models (1) and (2) as discussed in Section III-C.

2) Inter-channel interference derivation: When SPD functions are derived, the chosen M nodes report them to node u, which in turn distributes its SPD function to all the nodes in $\cup_x I_u^{(x)}$. Once a node obtains the SPD function, the derivation of inter-channel interference model is straightforward. Specifically, if channels x' and y' are strongly overlapping, node w can derive the interference on channel y' induced by interferer u on channel x' with power level P_z as:

$$RSS(u^{(x')}, w^{(y')}, P_z)_{dBm} = f_u(x',y',z)_{dBm} - PL_{y'}(u,w) \quad (6)$$

Similarly, if channels x' and y' are weakly overlapping, node w can derive the interference on channel y' that is induced by interferer u on channel x' with given quantile α as:

$$RSS(u^{(x')}, w^{(y')}, \alpha)_{dBm} = g_u(x',y',\alpha)_{dBm} - PL_{y'}(u,w) \quad (7)$$

We note that, as both SPD functions and path losses have been measured, node w can derive $RSS(u^{(x')}, w^{(y')}, P_z)$ or $RSS(u^{(x')}, w^{(y')}, \alpha)$ for any channel combination (x', y') without channel switching.

The pseudo code of the SPD-based interference measurement algorithm is shown in Algorithm 1.

B. Complexity analysis

We now briefly analyze the complexity of multi-channel interference measurement and the advantage of our mechanism. For the convenience of discussion, we define that, for a given sender u and its interference sets of all channels, measuring its signal attenuation model (Eq. (1) or (2)) of a given channel pair (x,y) for all nodes in $I_u^{(x)}$ incurs a complexity of $O(1)$, where x and y are sending and receiving channels respectively. Given that there are M overlapping channels, there are total M^2 possible combinations of sender/receiver channel pairs. The complexity of measuring the inter-channel interference induced by sender s

[1]Here we assume $|I_u^{(x)}| \geq M$ for all channels. When $|I_u^{(x)}| < M$, a node may be chosen to measure the path loss of multiple channels.

Algorithm 1 SPD-based interference measurement algorithm at node u.

Input: $I_u^{(x)}$ for all channel x;
Output: Inter-channel interference models for all nodes v ($v \in \cup_x I_u^{(x)}$).

1: All nodes in $\cup_x I_u^{(x)}$ measure the path loss to u on all channels according to (3).
2: **for** each channel x **do**
3: Randomly choose M nodes in $I_u^{(x)}$ to measure inter-channel RSS model for each overlapping channel.
4: Each chosen node derives u's SPD function of channel x accroding to (4) and (5), and sends it to u.
5: **end for**
6: u distributes its SPD functions to all nodes in $\cup_x I_u^{(x)}$.
7: Each node in $\cup_x I_u^{(x)}$ derives inter-channel interference model according to (6) and (7).

is $O(M^2)$. Our analysis shows that the complexity of SPD-based measurement algorithm is $O(M)$ resulting in a M-order complexity reduction. The details of the analysis are omitted due to space limitation and can be found in [23].

V. Impact on link-level performance

We now apply our interference models to both link capacity analysis and channel assignment protocols. We develop a multi-channel link capacity model by integrating our inter-channel interference models into an existing analytical framework. Moreover, we extend two latest multi-channel sensor network protocols to utilize overlapping channels.

A. Multi-channel link capacity

In this section, we present a model to predict the throughput capacity of a link in the presence of inter-channel interference. Accurate link capacity prediction is critical to the performance of a number of wireless protocols such as congestion control, link/channel scheduling, and QoS-aware routing. The achievable capacity of a link is inherently impacted by the design of MAC. We first analyze the link capacity for the case where carrier sense is not available, which is typically assumed in TDMA protocols. We then extend the analysis for CSMA MACs with carrier sense.

1) Multi-channel link capacity without carrier sense: When there is no carrier sense, a transmitter can send at the maximum channel rate. The link capacity is thus equal to the product of radio bandwidth and the receiver PRR. Several recent studies [6][16][17] have been conducted to model the relationship between packet reception rate (PRR) and signal to interference and noise ratio (SINR). Once SINR of a receiver is known, the PRR can then be predicted using existing empirical PRR-SINR models[6][16][17].

Suppose node u_0 is transmitting packets to node v_0 using channel n and there exists k active links denoted by set $Z = \{(u_i^{(x)}, v_i^{(x)}, P_{zi}) \mid 0 \le i \le k\}$ where $u_i^{(x)}$, $r_i^{(x)}$, and P_{zi} represent the sender, receiver, and transmit power of active link i using channel x. For receiver $v_0^{(x)}$, the SINR can be computed by treating all transmissions from $u_i (i \neq 0)$ as interference:

$$SINR(v_0^{(x)})_{dB} = RSS(u_0^{(x)}, v_0^{(x)}, P_{z0})_{dBm} \quad - \\ 10\log_{10}\left(\sum_{Z, i!=0} 10^{\frac{RSS(u_i^{(x)}, v_0^{(y)}, P_{zi})}{10}} + 10^{\frac{N_{v0}^{(n)}}{10}}\right) \tag{8}$$

where $RSS(v_0^{(x)}, u_i^{(y)}, P_{zi})$ is the signal strength of the packets sent by u_i at transmit power P_{zi} using channel y, which can be computed from the RSS model (Eq. (1) and Eq. (2)) in Section III-C. And $N_{v0}^{(x)}$ is the noise strength at receiver v_0 on channel x.

Suppose $PRR_{v0}^{(x)}(\cdot)$ represents the PRR-SINR model for node v_0 on channel x, which can be created by existing methods in [6][16][17]. The PRR of the link from u_0 to v_0 on channel x can then be computed by applying the SINR given by Eq. (8) into the PRR-SINR model:

$$PRR(u_0^{(x)}, v_0^{(x)}) = PRR_{u0}^{(x)}(SINR(v_0^{(x)})) \tag{9}$$

2) Multi-channel link capacity with carrier sense: We now focus our analysis on the link capacity with carrier sense. Our analysis assumes B-MAC [14], although it is also applicable to several other low-power MACs such as S-MAC [24] and 802.15.4 with minor modifications. Our analysis follows the measurement-based modeling framework for single-channel links proposed in [6]. However, several major extensions were made, which include integrating a carrier sense model for B-MAC and the multi-channel RSS models.

We assume that the network consists of a set of active links, denoted by $Z = \{(u_i, v_i) | 0 \le i < k\}$, where u is the sender and v is the receiver. Given a saturated traffic pattern for each active link, i.e., all transmitters are always backlogged, our objective is to derive the capacity of link z_i while all links in $Z - \{z_i\}$ are active. Channel assignments and power allocation of the network are given *a priori*. Suppose $c(i)$ and $p(i)$ represent the channel and power assigned to link i respectively. Then the capacity of link i in the presence of a set of interferers $Z - \{z_i\}$ can be expressed as:

$$c_i|_{Z-\{z_i\}} = \frac{P}{P+H} \times B \times \sum_{Y \in \mathcal{P}(Z-z_i)} \left(PRR^Y(u_i^{c(i)}, v_i^{c(i)}) \times t_{\{z_i\} \cup Y}\right)$$

where B is the channel rate; P and H are the sizes of payload and header; $\mathcal{P}(S)$ is the power of set S; $PRR^Y(u_i^{c(i)}, v_i^{c(i)})$ is the packet reception ratio of link z_i when all links in $Z - z_i$ are transmitting concurrently, which is given by Eq. (9). Due to space limitation, the details of derivation are omitted and can be found in [23].

B. Extensions to multi-channel protocols

Recently, several channel assignment and multi-channel protocols [8][22] have been developed to improve the performance of WSNs. These protocols rely on *interference assessment* to guide the decision of channel assignments. However, they either assume an adequate number of orthogonal channels [8], or use impractical interference model for channel and interference assessment [22]. Moreover, they prohibit the use of partially overlapping channels. However, number of orthogonal channels is often small due to inter-channel interference. Consequently, nodes must compete for a small number of orthogonal channels, which likely results in the degradation of capacity in moderate- to large-size networks. In this subsection, we describe how to extend a channel assignment protocols [22] and a multi-channel MAC [8] based on our inter-channel interference models.

1) Extending the TMCP protocol: Wu et al. [22] developed the Tree-based Multi-Channel Protocol (TMCP) for Wireless Sensor Networks (WSNs). TMCP partitions the whole network into subtrees and allocates orthogonal channels to each subtree. However, TMCP relies on the protocol model to estimate interference, i.e., two nodes interfere with each other if their physical distance is smaller than a threshold. The size of a node's interference set is defined as *interference value*, which is then used to guides subsequent subtree partition. However, such a distance-based interference model is highly inaccurate in practice as shown by recent empirical studies [12].

We now describe an extended TMPC protocol, referred to as TMCP-I, which employs our inter-channel RSS models for interference assessment in subtree partition and channel allocation. Similar with TMCP, TMCP-I first applies the Breadth-First search to compute a fat tree rooted at the sink, and then executes channel allocation one by one level from the top to the bottom on the fat tree. For each node u, TMCP assigns channel c to minimize the total inter- and intra-tree *interference value*. Once channel c is assigned, a subtree T_c rooted at the node is formed. However, the notation of interference value is only applicable to the binary interference model. In TMCP-I, we change the channel allocation criteria to maximize the overall PRR:

$$c = arg\max \sum_{v \in \cup_{1 \le i \le k} T_i} PRR(v, p_v) \tag{10}$$

where p_v is v's parent on its subtree, and $PRR(\cdot)$ is the PRR-SINR model described in Section V-A. k is the total number of subtrees found and T_i denotes the set of nodes on subtree i. We note that the computation of PRR accounts for the inter-channel interference among different trees. In addition, we also implemented a power control component in TMCP-I, which jointly sets the transmit power and channel of each node in order to maximize the total throughput.

In summary, TMCP-I makes two key modifications to the original TMCP. First, we use the measurement-based RSS models instead of the impractical binary model to assess the inter-channel interference. Second, we use the PRR-SINR model to guide the subtree partition, which is more accurate than the interference value defined in TMCP.

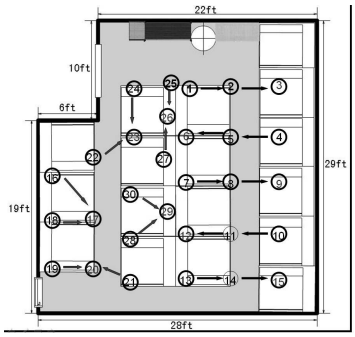

Figure 2. The test-bed used in the experiments. Each node is a TelosB mote equipped with CC2420 radio. The arrows represent the direction of data flows. Two different network topologies are constructed: motes 1-15 are grouped into three linear paths and motes 16-30 are grouped into 5 clusters with start topologies.

2) Extending the CM-MAC protocol: Le et al. [8] developed a MAC protocol which applies control theory to utilize multiple channels for WSNs. We refer to this protocol as control based multi-channel MAC (CM-MAC). The basic idea of CM-MAC is to partition the nodes into different sets and assign each an orthogonal home channel, while meeting the following constraints. First, communication within each set does not exceed the local capacity. Second, communication across sets is minimized. Le et al. [8] present a mechanism to allow cross-channel communication, and propose a dynamic algorithm to migrate home channel for each node when the old channel becomes overloaded. However, CM-MAC only uses orthogonal channels, whose number is typically small in practice.

We extend CM-MAC to utilize partially overlapping channels as follows. A new *channel assessment* component is added to provide accurate channel quality estimation and efficient home channel migration when the originally allocated channel becomes overloaded. We implemented the channel assessment component based on our inter-channel interference models. For an available channel, we predict the RSS for each transmitting neighbor and calculate the expected SINR. The home channel migrates when SINR of the new channel is higher than a threshold. We refer to the extended protocol as CM-MAC-I.

VI. Experimentation

We have implemented the components described in the previous sections in TinyOS-2.0.2 on TelosB motes. They include: 1) the RSS models for both strongly and weakly correlated channels described in Section III; 2) the lightweight interference measurement algorithm described in Section IV and 3) the extensions to two multi-channel protocols (TMCP-I and CM-MAC-I) described in Section V-B.

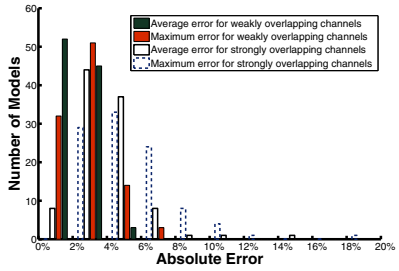

Figure 3. Accuracy of SPD algorithm.

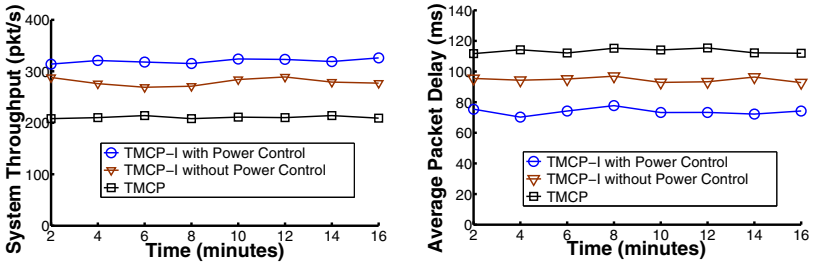

(a) System throughput

(b) Average packet delay

Figure 4. Evaluation of TMCP-I protocol.

Our test-bed is composed of 30 TelosB motes deployed in an office environment. The interference level of a network is inherently dependent on the topology. We constructed both linear and star topologies to evaluate the performance of our approach under different interference levels. Motes 1-15 are grouped into three linear paths and motes 16-30 are grouped into 5 clusters with star topologies.

A. Accuracy of SPD algorithm

We first evaluate the accuracy of the SPD-based interference measurement algorithm using four motes. Two motes serve as the sender and receiver, respectively. The third mote serves as jammer whose transmissions interfere with the packet reception of the receiver. The sender measures its spectral power density function by using the fourth mote. We vary the transmit power and channel of the jammer in order to create different interference conditions. In each setting, the SPD algorithm is executed to measure the receiver and jammer RSS models. We repeat this experiment in different settings to get a set of inter-channel RSS models for both strongly and weakly overlapping channels. In all experiments, a 90% quantile is used in the RSS model of weakly overlapping channels.

As a baseline, we implemented a simple algorithm in which the sender broadcasts 1000 packets on every channel and the receiver measures the RSS by reading the RSSI register. The background noise in RSSI values is filtered as described in Section III-A. We note that such a measurement method achieves high accuracy at the cost of significant measurement message overhead. Fig. 3 shows the distribution of maximum and average measurement error of SPD-based algorithm. The results are based on 100 samples for each type of models, i.e., inter-channel RSS models of strongly and weakly overlapping channels. It can be seen that the measurement of SPD is very accurate compared with the baseline algorithm. Specifically, the mean maximum error of SPD-based algorithm is 7.47%, and the mean average error is as low as 2.95%. However, as described in Section IV, the SPD algorithm incurs much lower overhead. In this experiment, SPD only broadcasts 50 measurement packets for each model.

B. Improvements of multi-channel protocols

We now evaluate the performance of TMCP-I protocols. Fig. 4 shows the average packet delay and system throughput of the TMCP and TMCP-I protocols on 15 motes. Four motes serve as sources with a maximum speed of 100 packets/second. In our implementation, TMCP uses 4 orthogonal channels while TMCP-I uses 8 channels in which every two of them are partially overlapping. We note that the total number of orthogonal (i.e., neither strongly nor weakly overlapping) channels on CC2420 is 4 in our experiments. We can see that TMCP-I (without power control) outperforms TMCP by about 50%. The power control component further improves the performance by about 10%. Fig. 4(b) shows the average packet delay measured for all packets in every two minutes. Consistent with the throughput results, TMCP-I with power control yields the minimum packet delay among the three protocols. TMCP-I without power control outperforms TMCP by around 25%. These results clearly demonstrate the advantage of using our inter-channel interference models.

We now evaluate the performance of CM-MAC-I using two different topologies shown in Fig. 2. The sources generate a packet in every 30 milliseconds. We run CM-MAC with 3 orthogonal channels (17, 19 and 21) as well as 6 channels (17 to 22) which are partially overlapping. CM-MAC-I used 6 overlapping channels. Fig. 5(a) shows that CM-MAC-I yields the minimum packet delay in all runs although some channels are overlapping. On the other hand, CM-MAC with overlapping channels can cause much longer delay (node 17 and 23) than with orthogonal channels. This is because CM-MAC is unaware of the interference between overlapping channels, which may result in severe contention at bottleneck nodes. This result shows that the existing multi-channels protocols cannot efficiently use overlapping channels. Fig. 5(b) and 5(c) show the throughput of different protocols on both cluster and linear topologies. It can be seen that CM-MAC-I yields the highest throughput in all runs. However, overlapping channels may not always lead to the improved throughput for CM-MAC. The throughput of line topologies is significantly lower than that of cluster topologies, due to the longer network paths. In summary, our RSS models

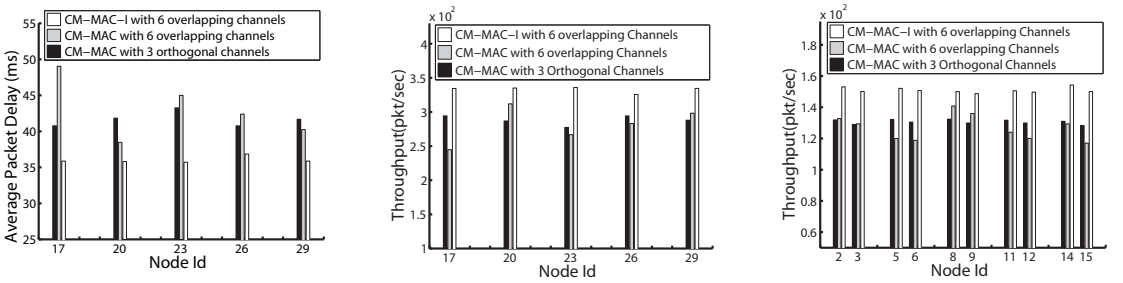

(a) Packet delay of different nodes with cluster topology

(b) Throughput of different nodes with cluster topology

(c) Throughput of different nodes with line topology

Figure 5. Evaluation of CM-MAC-I on both cluster and line topologies.

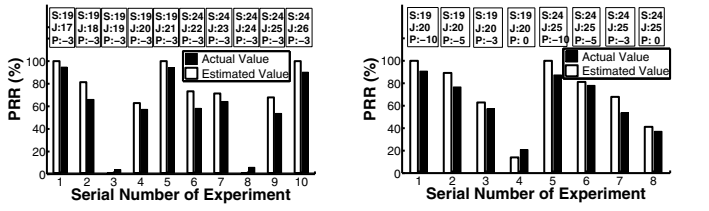

(a) Measured and predicted PRRs when the jammer uses different channels.

(b) Measured and predicted PRRs when the jammer uses different transmit power.

Figure 6. Measured and predicted link throughput without carrier sense. Each run is labeled by sender channel, jammer channel, and jammer transmit power.

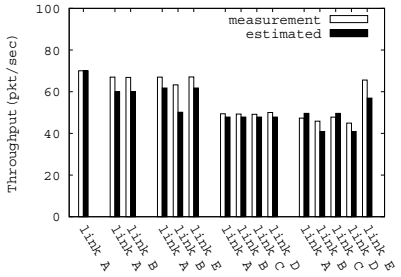

Figure 7. Measured and predicted link throughput with carrier sense.

can accurately predict the inter-channel interference allowing multi-channel protocols to take advantage of overlapping channels.

C. Accuracy of link capacity model

We now compare the measured PRR of links against the PRR predicted based on the RSS models. We integrate our RSS models into the PRR-SINR model proposed in [17]. The integrated model predicts the PRR of a link without carrier sense in the presence of inter-channel interference. The carrier sense of B-MAC is thus intentionally disabled. In Fig. 6(a) and 6(b), the data of each run is labeled by the sender channel, jammer channel, and jammer's transmit power. For instance, *S:19, J:17, P: -3* refer to the setting where the sender transmits on channel 19 and the jammer transmits on channel 17 with power -3 dBm. The transmit power of the sender is fixed to -3 dBm in all runs.

In Fig. 6(a), the jammer varies the channel from 17 to 26 while the sender uses channels 19 (columns 1 to 5) and 22 (columns 6 to 10). When the sender and jammer channels are close, the receiver experiences higher level of inter-channel interference resulting in lower PRRs. In particular, the PRR drops to near zero when they use the same channel. In Fig. 6(b), the jammer uses channels 20 and 25 while the sender uses the channel 19 and 24 with transmit power between -10 and 0 dBm. When the jammer increases transmit power, the receiver suffers higher level of inter-channel interference resulting in lower PRRs. When the jammer transmits at 0 dBm, the PRR drops to around 20%. In Fig. 6(a), the estimated values are slightly higher than the experimental results in most cases. This is because we use the average noise strength in SINR computation. However, the real noise yields sporadic high values due to the interference from environments [9]. Thus our model slightly overestimates PRR by ignoring the case where noise strength exceeds the average value, which will cause a packet loss. However, the average error between the measured and estimated PRRs is always within 9.76%. We note that the error is caused by the inaccuracy of both our RSS models and the PRR-SINR model proposed in [17].

We now evaluate the accuracy of our link capacity model with carrier sense. We randomly choose five links from the testbed topology, which start to transmit one by one. The RSS and PRR models are measured at the beginning of each run. Fig. 7 shows the measured and predicted throughput when the number of links increases from one to five. Links A and B use channel 17, links C and D use channel 18, and link E use channel 19. All links are saturated links and the packet size is 100 bytes. We note that these links use both strongly and weekly overlapping channels. We can see that the error of prediction is invisible when there are no more than 3 links. When there are more links, the interference among nodes is more complex resulting in higher prediction errors. In particular, our capacity model in Section V-A assumed that the transmissions from interfering links are precisely aligned, which is often impossible in practice due

to the unpredictable packet processing delays. As a result, the predicted SINR is higher than estimation resulting in slightly underestimation of link throughput. In the third set of experiment, throughput of link B drops when link E (using channel 19) joins the network. Since both link A and link E are strong interfering links of link B, link B has the lowest throughput. While the interference between links A and E is not strong enough to cause them to defer their transmissions, they have relative higher throughput. The overall average error between the predicted and measured PRRs is 6.8%.

VII. Conclusion

In this paper, we present a systematic study on the inter-channel interference and its impact on link capacity and the performance multi-channel protocols in LWNs. We develop practical models for capturing inter-channel signal attenuation and integrate them into both link capacity analysis and channel assignment protocols. We also propose a novel algorithm which can significantly reduce the overhead of multi-channel interference measurement by exploiting the spectral power density (SPD) of the transmitter. Our extensive experiments on a testbed of 30 TelosB motes show that 1) the SPD-based algorithm can accurately measure multi-channel interference with low overhead; 2) our link capacity model can accurately predict link throughput with and without carrier sense in the presence of multi-channel interference; 3) multi-channel protocols for LWNs can achieve significantly higher system throughput and lower communication delay by using overlapping channels.

References

[1] Cc2420 data sheet. In *http://www-inst.eecs.berkeley.edu/cs150/Documents/CC2420.pdf*.

[2] G. Brar, D. M.Blough, and P. Santi. Computationally efficient scheduling with the physical interference model for throughput improvement in wireless mesh networks. In *MobiCom*, 2006.

[3] C.-M. Cheng, P.-H. Hsiao, H. T. Kung, and D. Vlah. Adjacent channel interference in dual-radio 802.11a nodes and its impact on multi-hop networking. In *Globecom*, 2006.

[4] P. Fuxjager, D. Valerio, and F. Ricciato. The myth of non-overlapping channels: interference measurements in ieee 802.11. In *Wireless on Demand Network Systems and Services, WONS*, 2007.

[5] O. D. Incel, S. Dulman, P. Jansen, and S. Mullender. Multi-channel interference measurements for wireless sensor networks. In *LCN*, 2006.

[6] A. Kashyap, S. Ganguly, and S. R. Das. A measurement-based approach to modeling link capacity in 802.11-based wireless networks. In *MobiCom*, 2007.

[7] H. K. Le, D. Henriksson, and T. Abdelzaher. A control theory approach to throughput optimization in multi-channel collection sensor networks. In *IPSN*, 2007.

[8] H. K. Le, D. Henriksson, and T. Abdelzaher. A practical multi-channel media access control protocol for wireless sensor networks. In *IPSN*, 2008.

[9] H. Lee, A. Cerpa, and P. Levis. Improving wireless simulation through noise modeling. In *IPSN*, 2007.

[10] P. Li, N. Scalabrino, Y. Fang, E. Gregori, and I. Chlamtac. Channel interference in ieee 802.11b systems. In *Globecom*, 2007.

[11] S. Lin, J. Zhang, G. Zhou, L. Gu, T. He, and J. A. Stankovic. ATPC: Adaptive Transmission Power Control for Wireless Sensor Networks. In *SenSys*, 2006.

[12] R. Maheshwari, S. Jain, and S. R. Das. A measurement study of interference modeling and scheduling in low-power wireless networks. In *SenSys*, 2008.

[13] A. Mishra, V. Shrivastava, S. Banerjee, and W. Arbaugh. Partially overlapped channels not considered harmful. In *SIGMetrics*, 2006.

[14] J. Polastre, J. Hill, and D. Culler. Versatile low power media access for wireless sensor networks. In *SenSys*, 2004.

[15] L. Qiu, Y. Zhang, F. Wang, M. K. Han, and R. Mahajan. A general model of wireless interference. In *MobiCom*, 2007.

[16] C. Reis, R. Mahajan, M. Rodrig, D. Wetherall, and J. Zahorjan. Measurement-based models of delivery and interference in static wireless networks. In *Sigcomm*, 2006.

[17] M. Sha, G. Xing, G. Zhou, S. Liu, and X. Wang. C-mac: Model-driven concurrent medium access control for wireless sensor networks. In *Infocom*, 2009.

[18] J. So and N. Vaidya. Multi-channel mac for ad hoc networks:handling multi-channel hidden terminals using a single transceiver. In *MobiHoc*, 2004.

[19] D. Son, B. Krishnamachari, and J. Heidemann. Experimental study of concurrent transmission in wireless sensor networks. In *Sensys*, 2006.

[20] E. Toscano and L. L. Bello. Cross-channel interference in ieee 802.15.4 networks. In *WFCS*, 2008.

[21] E. G. Villegas, E. Lpez-Aguilera, R. Vidal, and J. Paradells. Effect of adjacent-channel interference in ieee 802.11 wlans. In *CrownCom*, 2007.

[22] Y. Wu, J. A. Stankovic, T. He, and S. Lin. Realistic and efficient multi-channel communications in wireless sensor networks. In *Infocom*, 2008.

[23] G. Xing, M. Sha, J. Huang, G. Zhou, X. Wang, and S. Liu. Multi-channel interference measurement and modeling in low-power wireless networks. Technical Report MSU-CSE-09-25, Computer Science and Engineering, Michigan State University, May 2009.

[24] W. Ye, J. Heidemann, and D. Estrin. An energy-efficient mac protocol for wireless sensor networks. In *Infocom*, 2002.

[25] G. Zhou, T. He, J. A. Stankovic, and T. F. Abdelzaher. Rid: radio interference detection in wireless sensor networks. In *Infocom*, 2005.